Nonlinear vibrational resonance

Shyamolina Ghosh and Deb Shankar Ray*
Indian Association for the Cultivation of Science, Jadavpur, Kolkata-700032, India

(Received 10 July 2013; published 9 October 2013)

We examine the nonlinear response of a bistable system driven by a high-frequency force to a low-frequency weak field. It is shown that the rapidly varying temporal oscillation breaks the spatial symmetry of the centrosymmetric potential. This gives rise to a finite nonzero response at the second harmonic of the low-frequency field, which can be optimized by an appropriate choice of vibrational amplitude of the high-frequency field close to that for the linear response. The potential implications of the nonlinear vibrational resonance are analyzed.

DOI: 10.1103/PhysRevE.88.042904 PACS number(s): 05.45.−a, 05.90.+m, 05.40.−a

I. INTRODUCTION

It is well-known that noise can play a constructive role in improving a weak signal in a nonlinear dynamical system. Stochastic resonance [1,2] is the first example of its kind, where the response of a bistable system to a weak deterministic signal gets enhanced by an external noise of optimal strength. Over the years the subject has grown in various directions with the observation of several variants of stochastic resonance and related phenomena in model zero-dimensional and spatially extended systems. The examples include, among others, resonant activation [3,4], coherence resonance [5,6], noise-induced transitions [7], pattern formation [8], and wave propagation [9].

An interesting related phenomenon analogous to stochastic resonance is vibrational resonance [10–17], which can occur when the noise is replaced by a high-frequency periodic force. Vibrational resonance is observed as resonant behavior of a response function of a nonlinear system driven by a high-frequency force toward a low-frequency signal. The first numerical observation by Landa and McClintock [10] has been corroborated by theory [11,12] and experiment [13–15] in analog electronic circuit and has been the subject of several subsequent investigations [16,17]. Vibrational resonance concerns linear response toward a weak probe field. An issue that, however, escaped the attention of the aforesaid investigations, to our knowledge, is the examination of nonlinear response of the system. The focus of the present paper is the observation of an interesting symmetry-breaking effect due to high-frequency force, manifested as a nonlinear response of the bistable system to a low-frequency field. We examine both over-damped and under-damped cases to show that the nonlinear response at the second harmonic of the low-frequency field can be optimized by the appropriate choice of the amplitude of the high-frequency field close to that for the linear response. The origin of the second harmonic generation, which is forbidden by virtue of possession of a center of symmetry, lies on the loss of spatial symmetry by high-frequency temporal oscillation. Keeping in view of its immediate relevance to nonlinear optics [18], we emphasize that the conspicuous feature of this phenomenon is the excitation of second harmonic in a centrosymmetric system in sharp contrast to second harmonic generation in strong laser field in a noncentrosymmetric environment. Because of these distinctive characteristics we refer to it as nonlinear vibrational resonance.

The role of symmetry breaking had been examined earlier in several related contexts. For example, Borromeo *et al.* [19] have pointed out that nonlinear mixing of additive and multiplicative zero-mean periodic or random signals can be effective in localizing a Brownian particle in one well of a symmetric double-well potential. The idea got an extension to noise rectification [20]. Furthermore, it has been shown [21] that stochastic resonance may occur in absence of symmetry breaking, which is a resonant synchronization effect of the switching mechanism, where nonlinearity plays a crucial role [22,23]. Another related issue is the control of transport in Brownian ratchet devices using nonlinear signal mixing of two incommensurate driving forces [22,24]. A common element of all these works is the presence of noise in additive or multiplicative form. The major and primary content of the present analysis is the realization of a resonance effect of nonlinear response in absence of stochasticity per se. Second, the symmetry breaking arises here due to the shift of steady state of the unperturbed dynamical system and therefore may be attributed to a nonlinear dynamical mechanism.

The paper is organized as follows: In Sec. II we derive the nonlinear response functions for an overdamped bistable oscillator and its extension to an underdamped situation. Theoretical estimates have been compared with the results of numerical simulations. The paper is concluded in Sec. III.

II. NONLINEAR RESPONSE AMPLITUDE

A. Overdamped oscillator

We consider vibrational resonance [10] in the simplest model of an overdamped bistable oscillator as described by the equation

$$\dot{x} - f(x) = c\cos(\omega t) + g\cos(\Omega t), \tag{2.1}$$

where $f(x) = -\frac{\partial V}{\partial x}$ and V(x) is a symmetric double-well potential of the form $V(x) = -\frac{1}{2}x^2 + \frac{1}{4}x^4$. $c\cos(\omega t)$ is the low-frequency input signal and $g\cos(\Omega t)$ corresponds to the rapidly oscillating periodic force with frequency $\Omega \gg \omega$. The linear response of the system is evaluated by calculating the sine and cosine components $B_s(\omega)$ and $B_c(\omega)$, respectively, of the output signal or the state of the system denoted by $x(t)$

*pcdsr@iacs.res.in

as follows:

$$B_s(\omega) = \frac{2}{nT}\int_0^{nT} x(t)\sin(\omega t),$$
$$B_c(\omega) = \frac{2}{nT}\int_0^{nT} x(t)\cos(\omega t), \tag{2.2}$$

where $T = \frac{2\pi}{\omega}$ with integer n. Solving Eq. (2.1) followed by extraction of its sine and cosine components yields the linear response function

$$Q_{\rm L}(\omega) = \sqrt{B_s^2(\omega) + B_c^2(\omega)}/c \tag{2.3}$$

and phase shift $\theta(\omega) = \tan^{-1}\{\frac{B_s(\omega)}{B_c(\omega)}\}$ of the response function with respect to input signal.

It is quite straightforward to extend the definition of linear response amplitude to nonlinear domain by calculating the sine and cosine components of $x(t)$ at the second harmonic frequency of the input signal,

$$B_s(2\omega) = \frac{2}{nT}\int_0^{nT} x(t)\sin(2\omega t),$$
$$B_c(2\omega) = \frac{2}{nT}\int_0^{nT} x(t)\cos(2\omega t), \tag{2.4}$$

where T is now redefined as $T = \frac{\pi}{\omega}$. Similarly, we may define the phase shift $\theta(2\omega) = \tan^{-1}\{\frac{B_s(2\omega)}{B_c(2\omega)}\}$ of the response function at the second harmonic frequency. The nonlinear response amplitude at the second harmonic can be determined by calculating

$$Q_{\rm NL}(2\omega) = \sqrt{B_s^2(2\omega) + B_c^2(2\omega)}/c^2. \tag{2.5}$$

We now emphasize a pertinent point at this stage. Because of the presence of inversion symmetry of the potential field $V(x)$ governing the dynamics Eq. (2.1), the response at 2ω, i.e., the second harmonic generation is forbidden in absence of high-frequency field ($g = 0$). In what follows we show that an optimal range of g can make the system respond at the second harmonic of the low-frequency field.

To obtain an appropriate theoretical estimate of the nonlinear response amplitude $Q_{\rm NL}(2\omega)$ we identify, following standard technique, two time scales of the dynamics and seek for a solution of the form

$$x = X(t,\omega t) + \psi(t,\Omega t). \tag{2.6}$$

Here $X(t,\omega t)$ and $\psi(t,\Omega t)$ correspond to the slow and the fast motion components, respectively. ψ is 2π periodic and therefore has zero mean as

$$\langle\psi(t,\tau)\rangle = \frac{1}{2\pi}\int_0^{2\pi}\psi(t,\tau)d\tau. \tag{2.7}$$

Here $\tau = \Omega t$ refers to the fast time scale. Making use of the decomposition Eq. (2.6) and averaging over the fast time scale we obtain, for slowly moving variable X,

$$\dot{X} - X + X^3 + 3X\langle\psi^2\rangle + 3X^2\langle\psi\rangle = c\cos(\omega t), \tag{2.8}$$

and for fast motion,

$$\dot{\psi} - \psi + \psi^3 + 3X[\psi^2 - \langle\psi^2\rangle] + 3X^2[\psi - \langle\psi\rangle] = g\cos(\Omega t), \tag{2.9}$$

ψ being a rapidly changing field we assume further $\dot{\psi} \gg \psi, \psi^2, \psi^3$. The dynamics of ψ can be written down as $\dot{\psi} = g\cos(\Omega t)$ so that its solution yields $\psi = \frac{g}{\Omega}\sin(\Omega t)$, $\langle\psi\rangle = \langle\psi^3\rangle = 0$ and $\langle\psi^2\rangle = \frac{1}{2}(\frac{g}{\Omega})^2$.

The motion of the slow component then becomes

$$\dot{X} - \alpha(g)X + X^3 = c\cos(\omega t), \tag{2.10}$$

where, $\alpha(g) = 1 - \frac{3}{2}(\frac{g}{\Omega})^2$.

A look into Eq. (2.10) reveals that the effect of high-frequency oscillation due to rapidly changing force $g\cos(\Omega t)$ in Eq. (2.1) is included in $\alpha(g)$. Equation (2.10) describes the over-damped dynamics of a particle in a double-well potential where the potential is modified by the strength and frequency of the high-frequency field. The steady states of the system are $X_s = 0$ for $g \geqslant \sqrt{\frac{2}{3}}\Omega$ and $X_s = \pm\sqrt{1 - \frac{3}{2}(\frac{g}{\Omega})^2}$ for $g < \sqrt{\frac{2}{3}}\Omega$. Thus, the fixed points can be controlled by the ratio $(\frac{g}{\Omega})$ of the rapidly varying field. The evolution of the dynamics around the steady state can be determined by introducing the perturbation variable $Y = X - X_s$, so that Eq. (2.10) becomes

$$\dot{Y} + 2\alpha(g)Y + 3X_sY^2 + Y^3 = c\cos(\omega t). \tag{2.11}$$

We now emphasize two pertinent points. First, we do not consider here the perturbation to be small. This makes it possible to calculate the nonlinear response of the system. Second, a comparison between Eqs. (2.1) and (2.11) shows that the center of symmetry of the potential $V(x)$ is destroyed in the effective dynamics of Y due to the appearance of the term $3X_sY^2$ for $g < \sqrt{\frac{2}{3}}\Omega$, which assures a nonzero value of the steady state X_s. The effective potential corresponding to slow motion away from equilibrium is described by $V_{\rm eff}(Y) = \alpha Y^2 + X_sY^3 + \frac{1}{4}Y^4$. The loss of symmetry arises due to the interference of high-frequency temporal oscillation and as we show here, allows us to calculate the response of the system at the second harmonic of the low-frequency probe in addition to the usual linear response function. An inspection of Eq. (2.11) shows that the term $3X_sY^2$ gives rise to a component oscillating at 2ω. Therefore, we assume the solution for $Y(t)$ in the form

$$Y(t) = k_1\cos(\omega t) + k_2\sin(\omega t) + k_3\cos(2\omega t) + k_4\sin(2\omega t). \tag{2.12}$$

Substituting the last expression into Eq. (2.11) and equating the coefficients of $\cos(\omega t)$, $\sin(\omega t)$, $\cos(2\omega t)$, and $\sin(2\omega t)$, we finally obtain

$$Y(t) = Y_{\rm L}(t) + Y_{\rm NL}(t), \tag{2.13}$$

where

$$Y_{\rm L} = A\cos(\omega t - \gamma) \quad \text{and} \quad Y_{\rm NL} = B\cos(2\omega t - \phi), \tag{2.14}$$

and

$$A = \sqrt{k_1^2 + k_2^2} = \frac{c}{\sqrt{\omega^2 + \{2\alpha(g)\}^2}}. \tag{2.15}$$

The usual linear response amplitude is given by

$$Q_{\rm L}(\omega) = \frac{A}{c} = \frac{1}{\sqrt{\omega^2 + \{2 - 3\,(g/\Omega)^2\}^2}}. \tag{2.16}$$

The nonlinear response $Y_{\mathrm{NL}}(t)$, on the other hand, assumes a similar form:

$$Y_{\mathrm{NL}} = B\cos(2\omega t - \phi), \tag{2.17}$$

where

$$B = \sqrt{k_3^2 + k_4^2} = \frac{(3X_s/2)\,c^2}{\sqrt{(2\omega)^2 + \{3c^2/2 + 2\alpha(g)\}^2}}. \tag{2.18}$$

The response amplitude at the second harmonic is therefore given by

$$Q_{\mathrm{NL}}(2\omega) = \frac{B}{c^2} = \frac{(3X_s/2)}{\sqrt{(2\omega)^2 + \{(3c^2/2) + 2 - 3\,(g/\Omega)^2\}^2}}. \tag{2.19}$$

We now discuss some notable features of the nonlinear vibrational resonance:

(i) The expressions for linear and second harmonic response amplitudes $Q_{\mathrm{L}}(\omega)$ and $Q_{\mathrm{NL}}(2\omega)$ show that the resonances appear at nearly the same values of g since the magnitude of $\frac{3}{2}c^2$ is small.

(ii) A quantity of interest is the ratio of the relative magnitudes of the linear to nonlinear response amplitudes. It appears that the ratio $\frac{Q_{\mathrm{L}}(\omega)}{Q_{\mathrm{NL}}(2\omega)} \sim \frac{1}{X_s}$, for $g < \sqrt{\frac{2}{3}}\Omega$. This implies that the magnitude of the nonlinear response is ameable to experimental investigation for the same set of parameters for which the linear response is studied.

(iii) Another distinctive feature of the nonlinear response is the following. The traditional way of generating second harmonic response is to use ultrastrong field in a noncentrosymmetric environment. In the present case, the second harmonic frequency is generated for the weak probe field in a centrosymmetric environment, where the loss of spatial symmetry originates from the high-frequency temporal oscillation.

In order to confirm our theoretical observations, we have carried out direct numerical simulation of Eq. (2.1). The representative results are shown for linear and nonlinear response amplitude by solid lines in Figs. 1(a) and 1(b), respectively, for different values of Ω; the fixed set of parameters used are $\omega = 0.1$ and $c = 0.01$. The variations of the linear response amplitude $Q_{\mathrm{L}}(\omega)$ [Eq. (2.3)] and the second harmonic response amplitude $Q_{\mathrm{NL}}(2\omega)$ [Eq. (2.5)] with amplitude g of the high-frequency force demonstrate the resonant behavior for optimal values of g. These numerical results are compared with the corresponding analytical estimates of $Q_{\mathrm{L}}(\omega)$ [Eq. (2.16)] and $Q_{\mathrm{NL}}(2\omega)$ [Eq. (2.19)] as shown by

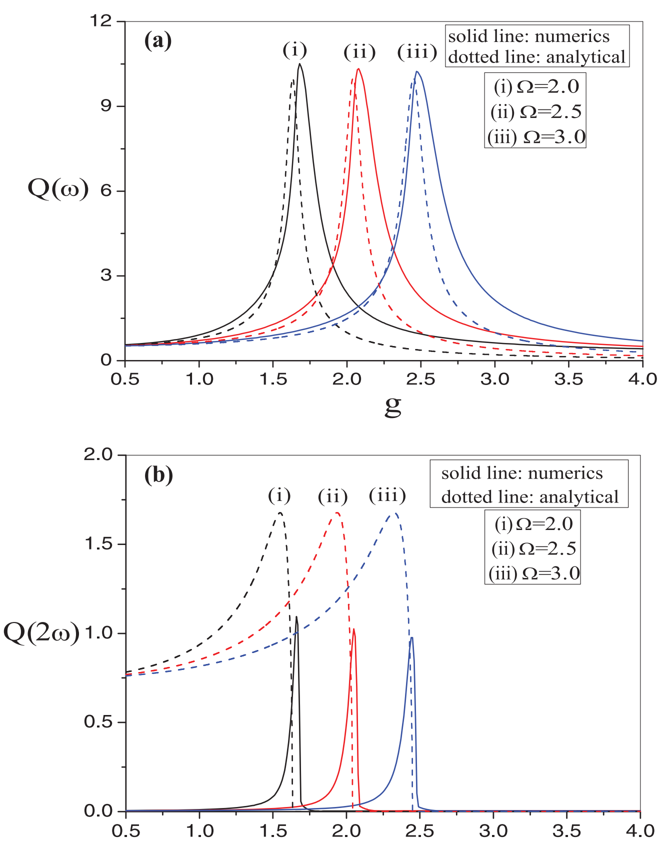

FIG. 1. (Color online) (a) Linear response amplitude $Q(\omega)$ and (b) nonlinear response amplitude $Q(2\omega)$ of the overdamped bistable system to low-frequency signal $c\cos(\omega t)$ under the influence of high-frequency vibrational force $g\cos(\Omega t)$ for three values of Ω and for a fixed parameter set $c = 0.01$ and $\omega = 0.1$. Numerical simulation results are based on Eqs. (2.1), (2.3), and (2.5); analytical estimates are based on Eqs. (2.16) and (2.19).

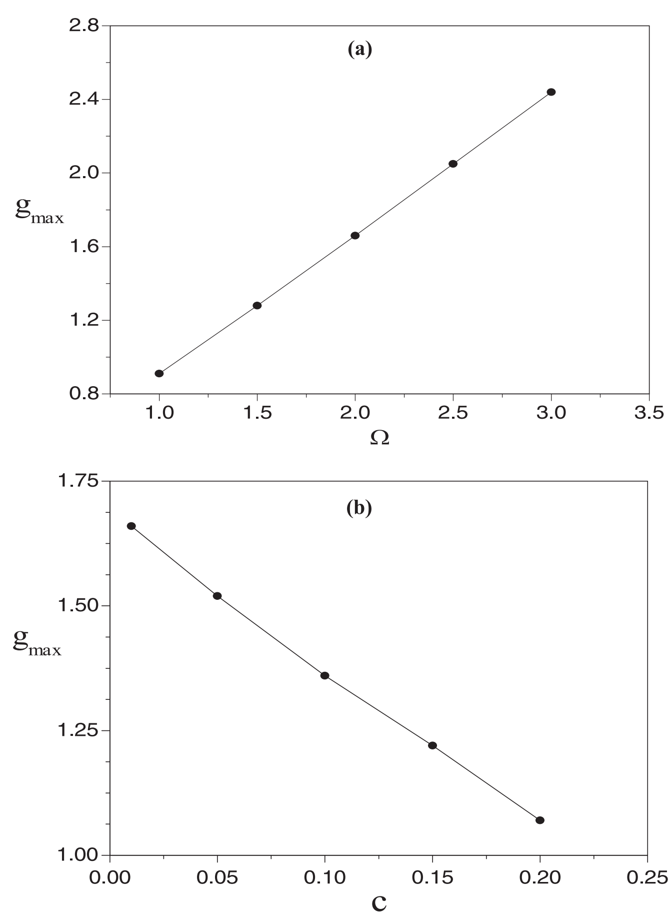

FIG. 2. Numerical results on the variation of the position of the maximum $g_{\max}$ of the second harmonic response amplitude of the overdamped bistable system (a) as a function of high frequency Ω for $c = 0.01$ and $\omega = 0.1$, (b) as a function of low-frequency signal amplitude c for $\omega = 0.1$ and $\Omega = 2.0$.

dotted lines in Figs. 1(a) and 1(b). The agreement is found to be fairly satisfactory. In Figs. 2(a) and 2(b), we have shown the numerical results on the dependence of the positions of the maximum amplitude ($g_{\max}$) on Ω and c for nonlinear response amplitude $Q_{\mathrm{NL}}(2\omega)$. The variations are qualitatively similar to what is seen in the corresponding variations for the linear response amplitude $Q_{\mathrm{L}}(\omega)$.

B. Underdamped oscillator

The above analysis can be extended to establish that nonlinear vibrational resonance can arise also in underdamped systems. To this end we consider

$$\ddot{x} + 2\delta\dot{x} - x + x^3 = c\cos(\omega t) + g\cos(\Omega t), \qquad (2.20)$$

where δ is a positive damping constant. We proceed as before. By separating x into the fast and slow motion components $\psi(t,\Omega t)$ and $X(t,\omega t)$, respectively, we derive the effective dynamics of X after averaging over high-frequency oscillations:

$$\ddot{X} + 2\delta\dot{X} - \beta(g)X + X^3 = c\cos(\omega t), \qquad (2.21)$$

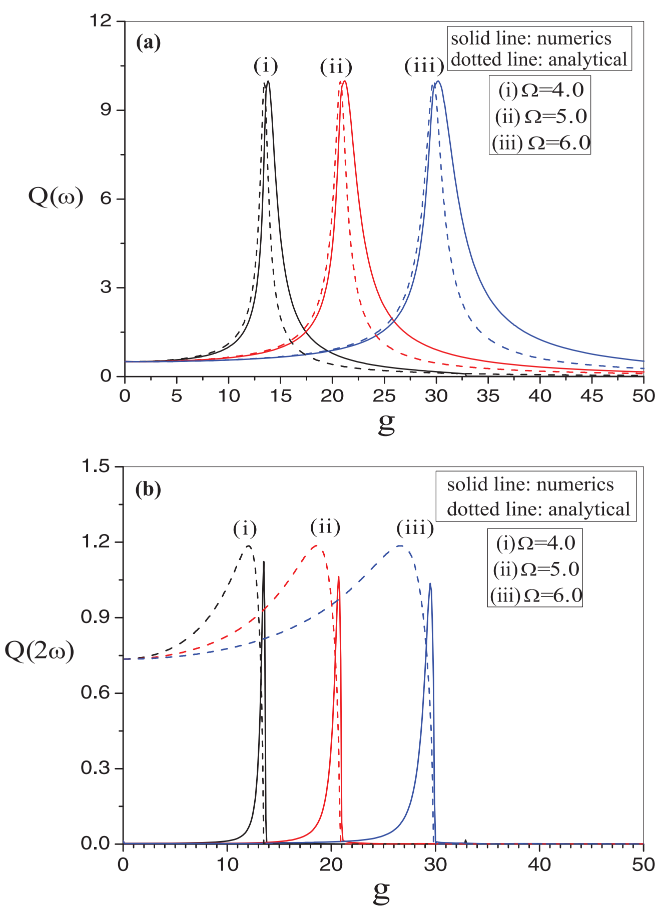

FIG. 3. (Color online) (a) Linear response amplitude $Q(\omega)$ and (b) nonlinear response amplitude $Q(2\omega)$ of the underdamped system to low-frequency periodic signal $c\cos(\omega t)$ under the influence of high-frequency vibrational force $g\cos(\Omega t)$ for three values of Ω and for a fixed parameter set $c = 0.01$, $\omega = 0.1$, and $\delta = 0.5$. Numerical simulation results are based on Eqs. (2.20), (2.3), and (2.5); analytical estimates are based on Eqs. (2.24) and (2.25).

where

$$\beta(g) = 1 - 3\langle\psi^2\rangle \quad \text{and} \quad \langle\psi^2\rangle = \frac{g^2}{2}\left[\frac{1+(2\delta/\Omega)^2}{\{(2\delta)^2+\Omega^2\}^2}\right]. \qquad (2.22)$$

The steady states X_s of the dynamics are now modified as $X_s = 0$ for $g \geqslant \sqrt{\frac{2}{3}[\frac{\{(2\delta)^2+\Omega^2\}^2}{1+(2\delta/\Omega)^2}]}$ and $X_s = \pm\sqrt{\beta(g)}$ for $g < \sqrt{\frac{2}{3}[\frac{\{(2\delta)^2+\Omega^2\}^2}{1+(2\delta/\Omega)^2}]}$. The equation for the deviation from the steady state, Y is given by

$$\ddot{Y} + 2\delta\dot{Y} + 2\beta(g)Y + 3X_sY^2 + Y^3 = c\cos(\omega t). \qquad (2.23)$$

By using the solution of Eq. (2.12), it is quite straightforward to calculate the linear and nonlinear amplitudes $Q_{\mathrm{L}}(\omega)$ and $Q_{\mathrm{NL}}(2\omega)$, respectively:

$$Q_{\mathrm{L}}(\omega) = \frac{A}{c} = \frac{1}{\sqrt{(2\delta\omega)^2 + \{2\beta(g)-\omega^2\}^2}} \qquad (2.24)$$

and

$$Q_{\mathrm{NL}}(2\omega) = \frac{B}{c^2} = \frac{(3X_s/2)}{\sqrt{(2\omega)^2(1+2\delta)^2 + \{2\beta(g)\}^2}}. \qquad (2.25)$$

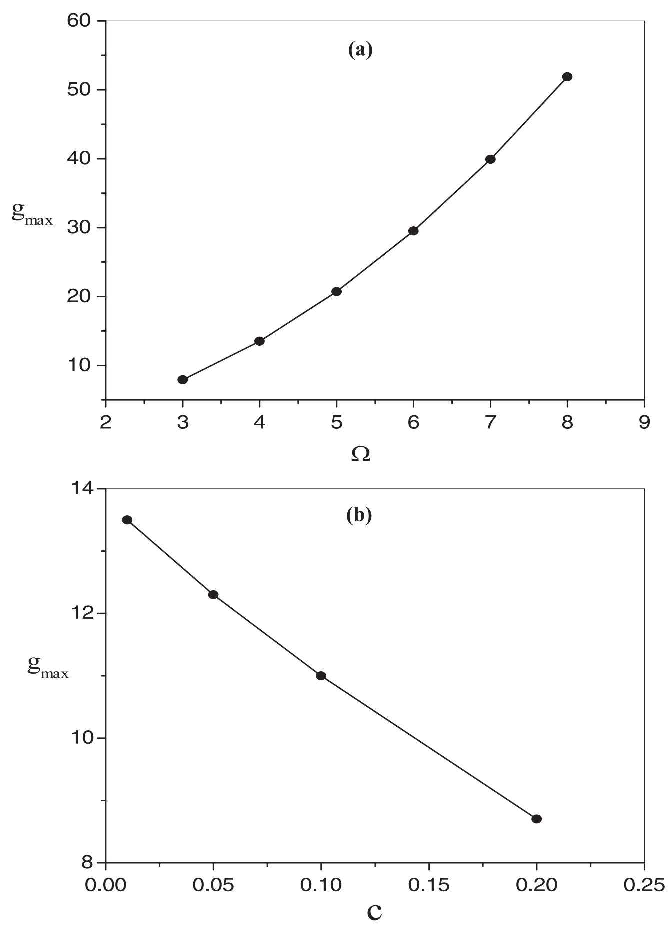

FIG. 4. Numerical variation of the position of the maximum $g_{\max}$ of the second harmonic response amplitude (a) as a function of high-frequency Ω for $c = 0.01$, $\omega = 0.1$, and $\delta = 0.5$, and (b) as a function of low-frequency signal for $\omega = 0.1$, $\Omega = 4.0$, and $\delta = 0.5$.

In Figs. 3(a) and 3(b) we show the numerical simulation results (solid lines) on the linear and nonlinear response amplitudes of the underdamped system [Eq. (2.20)] given by Eqs. (2.3) and (2.5), respectively, to varying amplitude of the high-frequency field, g for a fixed set of parameters: $c = 0.01$, $\omega = 0.1$, and $\delta = 0.5$. The responses clearly reveal the resonant behavior as expected from theoretical results depicted by dotted lines in Figs. 3(a) and 3(b). The agreement is found to be quite satisfactory. Figure 4(a) shows that the numerical variation of $g_{\max}$ (for nonlinear response amplitude) with Ω for $c = 0.01$, $\omega = 0.1$, and $\delta = 0.5$ is very weakly nonlinear. The variation of $g_{\max}$ with c is illustrated in Fig. 4(b) for the parameter set $c = 0.01$, $\Omega = 4.0$, and $\delta = 0.5$. The dependence is found to be relatively stronger compared to the over-damped case. A further comparison between the second harmonic response amplitudes [Eqs. (2.19) and (2.25)] for the overdamped and underdamped cases shows the absence of explicit dependence of probe amplitude in the resonance denominator in the underdamped situation.

Before conclusion, we emphasize that the origin of the nonlinear vibrational resonance lies on effective reduction of stiffness of the oscillator induced by high-frequency oscillation as in the case of usual vibrational resonance. This reduction results in amplification of the weak signal not only at the fundamental frequency but also at the higher harmonic frequency.

III. CONCLUSION

The essence of vibrational resonance is the amplification of weak low-frequency signal by a nonlinear system driven by a high-frequency force. We have extended this idea to show that the excitation of the system can be made even at the second harmonic of the low-frequency signal. The nonlinear response at the second harmonic is crucially dependent on the noncentrosymmetric nature of the underlying potential. In nonlinear optics the traditional way of generation of second harmonic is to use degenerate three-wave mixing in a noncentrosymmetric medium where a strong pump field with a frequency excites the medium at its second harmonic. The present scenario, however, is clearly distinct on two accounts. First, a high-frequency field can destroy the center of symmetry of the centrosymmetric medium. Second, because of reduction of stiffness, which makes the system more polarizable, the low-frequency signal can excite the medium at the second harmonic of the weak field for an optimal strength of the high-frequency field. In view of these considerations, we conclude this paper by suggesting an interesting application of the results presented above to nonlinear optics. We envisage a (high-frequency) pump and (low-frequency) probe set up for the present purpose. A suitable centrosymmetric crystal can be made to interact with the pump field. The secondary radiation due to nonlinear polarization can be detected by the weak probe at its second harmonic. To observe the resonance it is necessary to tune the strength of the pump field over an appropriate range. Nonlinear vibrational resonance has thus promising implications in nonlinear optics.

ACKNOWLEDGMENT

Thanks are due to the Council of Scientific & Industrial Research, Government of India, for partial financial support.

[1] R. Benzi, A. Sutera, and A. Vulpiani, J. Phys. A: Math. Gen. **14**, L453 (1981); B. McNamara, K. Wiesenfeld, and R. Roy, Phys. Rev. Lett. **60**, 2626 (1988).
[2] L. Gammaitoni, F. Marchesoni, E. Menichella-Saetta, and S. Santucci, Phys. Rev. Lett. **62**, 349 (1989); V. I. Melnikov, Phys. Rev. E **48**, 2481 (1993); L. Gammaitoni, P. Hänggi, P. Jung, and F. Marchesoni, Rev. Mod. Phys. **70**, 223 (1998).
[3] C. R. Doering and J. C. Gadoua, Phys. Rev. Lett. **69**, 2318 (1992); M. Marchi, F. Marchesoni, L. Gammaitoni, E. Menichella-Saetta, and S. Santucci, Phys. Rev. E **54**, 3479 (1996).
[4] Rosario N. Mantegna and B. Spagnolo, Phys. Rev. Lett. **84**, 3025 (2000); P. K. Ghosh and D. S. Ray, J. Chem. Phys. **125**, 124102 (2006); A. Fiasconaro and B. Spagnolo, Phys. Rev. E **83**, 041122 (2011).
[5] Arkady S. Pikovsky and J. Kurths, Phys. Rev. Lett. **78**, 775 (1997); D. E. Postnov, S. K. Han, T. G. Yim, and O. V. Sosnovtseva, Phys. Rev. E **59**, R3791 (1999).
[6] G. Giacomelli, M. Giudici, S. Balle, and J. R. Tredicce, Phys. Rev. Lett. **84**, 3298 (2000); K. Miyakawa and H. Isikawa, Phys. Rev. E **66**, 046204 (2002).
[7] W. Horsthemke and R. Lefever, Phys. Letts. A **64**, 19 (1977); C. Van den Broeck, J. M. R. Parrondo, and R. Toral, Phys. Rev. Lett. **73**, 3395 (1994); P. K. Ghosh, D. Barik, and D. S. Ray, Phys. Letts. A **342**, 12 (2005).
[8] F. Sagués, J. M. Sancho, and J. García-Ojalvo, Rev. Mod. Phys. **79**, 829 (2007); J. Buceta, M. Ibañes, J. M. Sancho, and K. Lindenberg, Phys. Rev. E **67**, 021113 (2003); A. Sanz-Anchelergues, A. M. Zhabotinsky, I. R. Epstein, and A. P. Muñuzuri, *ibid.* **63**, 056124 (2001); S. Dutta, S. S. Riaz, and D. S. Ray, *ibid.* **71**, 036216 (2005); D. Das and D. S. Ray, *ibid.* **87**, 062924 (2013); B. Spagnoloa and A. La Barbera, Physica A **315**, 114 (2002).
[9] S. Alonso, I. Sendiña-Nadal, V. Pérez-Muñuzuri, J. M. Sancho, and F. Sagués, Phys. Rev. Lett. **87**, 078302 (2001).
[10] P. Landa and P. McClintock, J. Phys. A **33**, L433 (2000).
[11] C. Jeevarathinam, S. Rajasekar, and M. A. F. Sanjuán, Phys. Rev. E **83**, 066205 (2011).
[12] W. Can-Jun, Chin. Phys. Lett. **28**, 090504 (2011).
[13] A. A. Zaikin, L. López, J. P. Baltanás, J. Kurths, and M. A. F. Sanjuán, Phys. Rev. E **66**, 011106 (2002).
[14] J. P. Baltanás, L. López, I. I. Blechman, P. S. Landa, A. Zaikin, J. Kurths, and M. A. F. Sanjuán, Phys. Rev. E **67**, 066119 (2003).
[15] V. N. Chizhevsky, E. Smeu, and G. Giacomelli, Phys. Rev. Lett. **91**, 220602 (2003).
[16] J. Casado-Pascual and J. P. Baltanás, Phys. Rev. E **69**, 046108 (2004).

[17] V. N. Chizhevsky and Giovanni Giacomelli, Phys. Rev. E **73**, 022103 (2006).

[18] R. W. Boyd, *Nonlinear Optics*, 3rd ed. (Academic Press, New York, 2008).

[19] M. Borromeo and F. Marchesoni, Europhys. Lett. **68**, 783 (2004); Phys. Rev. E **71**, 031105 (2005).

[20] M. Borromeo, S. Giusepponi, and F. Marchesoni, Phys. Rev. E **74**, 031121 (2006).

[21] L. Gammaitoni, F. Marchesoni, and S. Santucci, Phys. Lett. A **195**, 116 (1994).

[22] S. Savel'ev, F. Marchesoni, P. Hänggi, and F. Nori, Europhys. Lett. **67**, 179 (2004).

[23] F. Marchesoni, Phys. Lett. A **119**, 221 (1986).

[24] M. Borromeo and F. Marchesoni, Phys. Rev. E **73**, 016142 (2006); I. I. Blekhman, *Vibratianal Mechanics* (World Scientific, Singapore, 2000).